Robotica (2011) volume 29, pp. 917–927. © Cambridge University Press 2011
doi:10.1017/S0263574711000130

Robot accuracy evaluation using a ball-bar link system

Yeon Taek Oh*

Mechatronics & Manufacturing Technology Center, Samsung Electronics Co., Ltd., Suwon, Korea

(Received in Final Form: February 5, 2011. First published online: March 15, 2011)

SUMMARY
Relatively large errors can exist in industrial robots as a result of mismatch between the controller model and the corresponding physical model. The paper outlines a novel approach for accuracy assessment and adjustment of multiaxis industrial robots through a low-cost ball-bar link system. The features of the ball-bar, which incorporated a 12 mm range digital displacement transducer in conjunction with a PC, are discussed. The ball-bar device was used in both a trammelling and circular mode of operation. This produced data which not only related to the accuracy of the robot but also enabled joint errors to be significantly reduced.

KEYWORDS: Robot calibration; Ball-bar; Robot accuracy; Robot modelling; Angle error

1. Introduction

Robots are being used in many areas where accuracy and kinematic performance can be crucial, for example, in part assembly, cleaning and deburring, drilling, welding, etc. These operations generally require performance and accuracy greatly exceeding that was needed on earlier robot system.

The major robot performance constraints are repeatability and accuracy, following by uptime, load capacity, velocity and size of robot. The specifications quoted by the manufacturers are generally not sufficient to determine the process capability of the robot required. Most of the time, manufacturers specify resolution and repeatability rather than accuracy, but accuracy is important for offline programming and process planning. Robots from the same production batch, with identical specifications, can demonstrate different characteristics when operated under different conditions (different loads, speeds, durations, temperature, etc.). Standardised testing and evaluation techniques are needed to examine the process capability of a wide variety of robots in order to make the appropriate selection. During their life, robots may require maintenance which may involve changing encoders, etc. Unless a redatuming technique is available then the accuracy could differ significantly from that achieved prior to the maintenance. To achieve the previous performance, reteaching or redatuming may be required.

Robot calibration is a term applied to the procedure used in determining actual values which describe the geometric dimensions and mechanical characteristics of a robot. Robot calibration plays an increasingly important role in robot production as well as in robot implementation and operation within computer integrated manufacturing or assembly systems. The production, implementation and operation of robots are all areas where robot calibration results can lead to significant accuracy improvement. Many robot calibration methods have been introduced.[1–3,16,17]

One of the first pose measurement devices, made by R. H. McEntire[4] is an arrangement of three pairs of dial gauges, which detect three mutually perpendicular faces of a cube, held in the end effector. Research by P. G. Ranky[5] follows the original concept of attaching a cube to the robot end effector and describes a pose measurement device utilising nine dial gauges. This method has been improved by replacing the dial gauge with nine Linear Variable Differential Transformer (LVDT) and a cube, by D. L. Riley.[6] Six degrees of freedom pose measurement and calibration test stand was built. With pose determination, the test stand had the ability to determine information on both the repeatability and accuracy. These systems impose a physical restriction in that the robot must be moved slowly when the cube is within the vicinity of the transducer. Thus repeatability of a point far away from the transducer cannot be measured.

Also accuracy is much more difficult to measure in a robot application. The three-cable method[7] measures distance and employs three cables under tension. The three cables, originating from the three fixed-cable feeding devices whose locations are measured, are tied to the robot wrist. By evaluating the length of each cable, the position of the robot wrist in the work zone may be readily obtained. The major limitation of the measurement technique is the sag errors resulting from the cable weight when the robot end effector is far away from the measurement station.

The popular commercial calibration method is a laser-tracking system which was developed by Lau.[8] This system demonstrated higher accuracy and faster measurement than other measuring systems, but hardware is complicated and expensive.

Subsequently, the use of a socketed ball bar to test measuring machines and machine tools was first introduced by Bryan.[9] Also a modified extensible ball bar having a radial travel of 50 mm was introduced by Vira and Lau.[10] The measurement direction was radial on a swept sphere but considered axial on the ball bar. Thus radius and length of the ball bar are interchangeable. At each end of the ball bar, a high-precision steel ball of 25.4 mm in diameter was attached. One end of the ball bar is attached to a magnetic socket which allows it to rotate freely, whilst the other end is mounted on the universal joint that is attached to the robot end

* E-mail: yeonoh63@hanmir.com

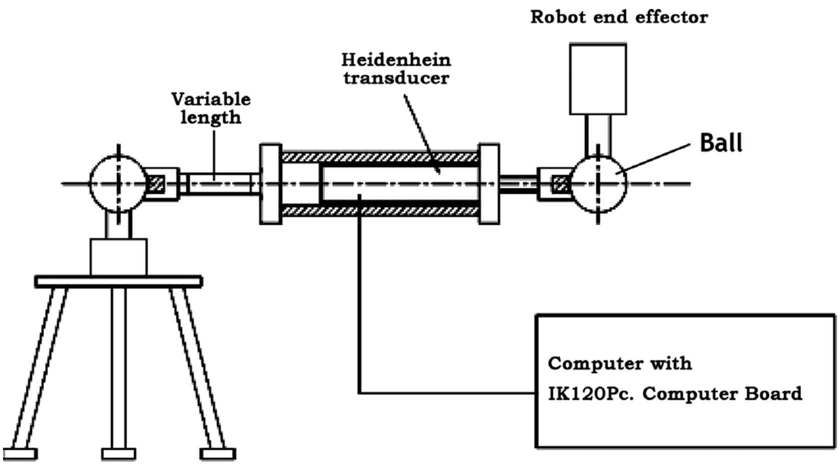

Fig. 1. System block diagram of robot calibration system.

effector. The probe is installed in the ball bar to measure the radial displacement between the two spheres. However this ball bar was only used on an arc path rather than a full circle because of the limitation of the joint mechanism between the extensible ball bar and the robot end effector. Thus the reference position of the arc centre cannot be defined with radial displacement data of the arc path in the coordination system of the robot working volume.

Consequently a new link system using a six-point kinematic design was developed by the author for measuring the positioning repeatability and accuracy and tested on the industrial robot because a six-point kinematic design can attain good repeatability and has good rigidity.[11] The aim of this research is to develop a strategy for the accuracy performance evaluation of industrial robots by using low-cost hardware in the form of ball bars. A new design for the kinematic link system will be investigated in order to overcome range and absolute length limitation with existing systems. The problem of interpretation of the data obtained from the new hardware will be investigated by simulating the kinematic model of the robot structure for 2, 3 and 6 degrees of freedom and comparing these with the experimental data obtained using this new hardware. The experimental verification of the strategy will be undertaken on a standard six axes industrial robot.

2. Principle of Ball Link System and Data Sampling

The ball-bar kinematic link system is well established for undertaking circular contouring test in computer numerical control (CNC) milling machine.[9,13,14] The initial design of the link is generally based on a flexible ball-bar concept using an LVDT. The LVDT is generally adequate for the error range encountered in machine tools but limited on the range for robot application due to the large error band of the industrial robot. Using the long measurement range of transducer, a light kinematic link system was developed for assessing the contouring capability (geometric error, robot drive system errors) of industrial robot.[15]

The origin of the circular contouring path is established by setting one reference ball coincidental with the centre of the second ball, i.e. the robot is programmed to move about a circular path with respect to its origin. Also the robot position is calculated with the inverse kinematic solution. The first ball is mounted on the robot end effector, with a second ball mounted in the working space of the robot.

The relative change in the distance between these two spheres during the circular contouring operation of the robot represents the radial error. This so called set-up error is inevitable when setting the origin between the two spheres, but its influence on the results can be easily eliminated with software analysis.

In order to carry out the contouring test on the robot, a ball is mounted on the robot end effector in place of a gripper, and a connecting kinematic link containing a Heidenhain transducer (Model: MT12(b), glass scale-type), whose specifications are given next, links this ball with a second ball, mounted on the magnetic base of the tripod. A magnetic base was used to minimise possible damage to the robot by incorrect programming and also to simplify the set-up. The deviations from nominal radius are established by setting the kinematic link against a calibrated setting fixture.

The robot is programmed to move around a circle with respect to the fixed ball held on the magnetic base. If the robot has no error, and there is zero set-up error between the balls, then no relative movement is detected by the Heidenhain transducer during the circular movement because the distance between the two balls remains constant. If the robot does not move in an ideal circle because of the influence of some error including the initial set-up, relative movement between the two balls can be measured and interpreted as a deviation from the nominal circular path.

Figure 1 shows this contouring measurement system comprising of a kinematic transducer link, and associated computer hardware, the kinematic contouring measurement system being interfaced with the computer. The output signal from the transducer is fed to an IK120 PC Counter Board in the computer, and the transferred data is analysed in terms of the deviation from the nominal circle.

2.1. Components

The system comprises of the following hardware specification.

Experimental equipment (design and link for the research)

- Kinematic transducer link and holder

Several different sizes of kinematic link bar were constructed for different test purposes. The length of the

https://doi.org/10.1017/S0263574711000130 Published online by Cambridge University Press

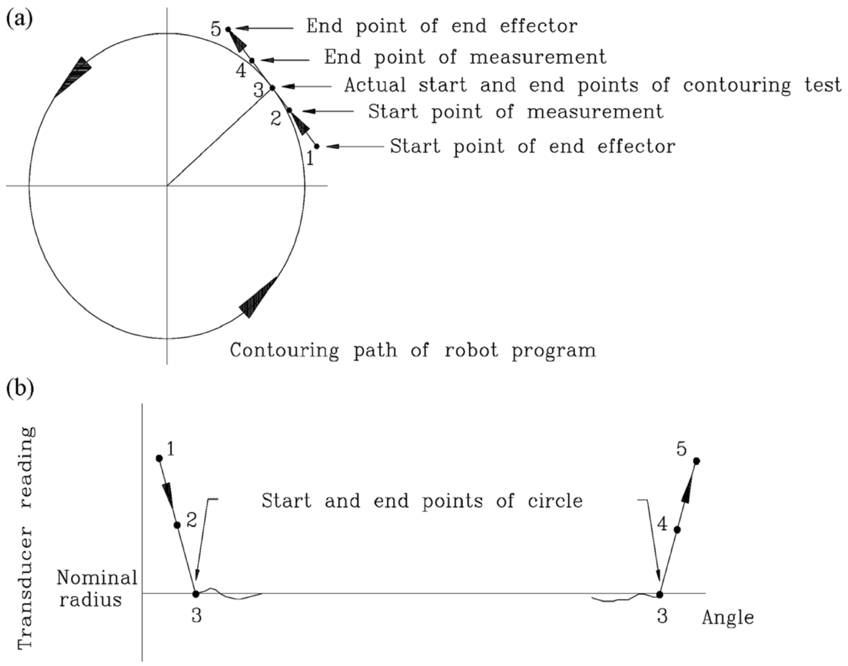

Fig. 2. Basic principles of sampling of start and end points.

link can be adjusted from 200 mm to 1000 mm by inserting simple extension pieces. The selection of the size of the link depends upon the purpose of the test.

- Transducer (Heidenhain Metro gauge MT 12(B))

  (a) Measuring standard: DIADUR glass scale with incremental grating, period 10 µm
  (b) Travel: 12 mm
  (c) Measuring resolution: ±0.5 µm
  (d) Permissible measuring velocity: 0.25 m/s (along the axis of the probe)

- Link setting fixture

  The centre distance between two balls: 200.017 mm
  Equipment

- PC and Interface card (IK120 PC Counter Board)

2.2. Construction of the kinematic link

2.2.1. Kinematic link. The kinematic link is shown in Fig. 1. The link is a lightweight construction from carbon fibre rod and aluminium alloy. In addition, the low coefficient of expansion of carbon fibre makes it thermally stable. The link is supported between two spheres. Alignment of the transducer link is facilitated by a magnetic clamping force on a three point contact with the ball. The master spheres are contacted directly by the three flat faces of a steel cup. With this arrangement, accuracy and repeatability can easily be achieved.

2.2.2. Linear measuring transducer. There are numerous types of commercially available transducers which are suitable for use with the robot calibration system. The Heidenhain transducer was used for this project because of its long measurement range of 12 mm.

2.2.3. Kinematic link setting fixture. This was constructed by mounting two balls in supports onto a stiff steel base. The balls were mounted onto the ball holding supports by high adhesive glue, and the ball holders are fitted to the thick square steel bar by tight fitting screws. The centre distance between the balls was calibrated using a coordinate measuring machine (CMM) machine.

2.3. Acquisition of experimental data

The transducer interface card was inserted in the motherboard of the computer so that the signal from the transducer could be read by the computer. The basic requirements of the sampling are as follows:

(1) Sampling must be uniform around the profile.
(2) Sufficient sampling data are required to display and analyse the error.
(3) The number of sampling data should be independent of contouring speed and link length.

To obtain the desired number of samples of data during the time of contouring, the Heidenhain interface card is read and a delay introduced before it is read again. The time response to read the card depends on not only the specified speed of the card but also on the speed of the computer. The required delay between readings often has a minimum value of 1 ms. The delay requirement was achieved by introducing a dummy 'do loop' into the program between consecutive read operations. To make the above sampling technique independent of the computer speed, etc., the 'do loop' is calibrated by the program. The required delay time is shown below.

$$\textit{Contouring time} = 2 \times \pi \times \textit{link length} \times 60/\textit{feedrate}$$

$$\textit{Delay time} = \textit{contouring time}/\textit{No. of sampling},$$

where *No. of sampling is the total required sampling number.*

Using this technique, Fig. 2 shows that sufficient samples can be achieved at the wider range of feed rate, computer speed and link length.

https://doi.org/10.1017/S0263574711000130 Published online by Cambridge University Press

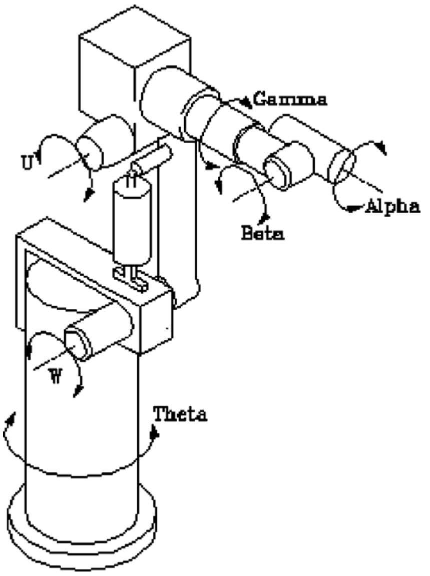

Fig. 3. Link coordination systems for the Fanuc robot.

2.4. Synchronisation of computer and robot controller

In order to analyse, the data from the transducer, the program must know the start and end point on the circular profile, i.e. the computer must know when to start and end the recording of transducer information. Also there are different response times between mechanical and electrical components.

Therefore the data synchronisation was performed by using software algorithms. This was based on the rapid change in the transducer output from the contouring motion. After starting the contouring, the reading of the transducer was not recorded by the computer until it was at the measuring range of the transducer.

During the test, the end effector is commanded to contour a straight line and a whole or part of a circular contour. As shown in Fig. 2(a) tangential approaching line to the test circle at the entry and exit point is introduced for software. The method to determine the start and end points is to check the slope of the output of the transducer reading. The slope is defined as the difference between two consecutive readings.

As soon as the contouring begins, the samples are not taken by the software until they are within a 2 mm radial distance from the tangent point on the circle. When the end effector approaches the ideal start point, the slope becomes gradually smaller and finally zero. A figure on the slope is set to determine the start point. The same method is used to find the end point. The use of the tangential approach path is designed to reduce the possible transient error.

3. Application to a Six Axes Industrial Robot

Figure 3 illustrates a consistent algorithm for the industrial robot arm used in the research. Also the ball-bar link system is used in the following two methods.

3.1. Trammelling technique

The perpendicularity of an axis in a milling machine with respect to the cutter spindle is measured by means of the trammel technique.[12] The dial gauge is fixed to the spindle and set within its range and the difference in reading noted when the spindle is rotated through 180°. If the spindle is square to the table, the deviation of the dial indicator will be zero. If not, the deviation will correspond to the squareness error. However, for robot applications, a reference plane is not readily available in the robot working space, and consequently an alternative technique must be adopted.

A trammel technique using the ball links was applied to the robot to measure the datum location error of the Beta axis. To facilitate these measurements, the base ball is initially set to the centre of the Gamma axis with the aid of the kinematic link as shown in Fig. 4. With the Beta axis set at nominally 90° to the Gamma axis, the kinematic link was located between the base ball and ball located at the robot end effector. In order to verify that the offset error between the base ball with respect to the centre of the Gamma axis has been minimised, the length between the base ball and ball located in the end effector was also measured by operating the robot in a fully contouring circle mode over a 360° rotation of the Gamma axis and a continuously sampling the change in the link length by the computer. The least squares centre of this continuous circular data represents the offset of the base ball.

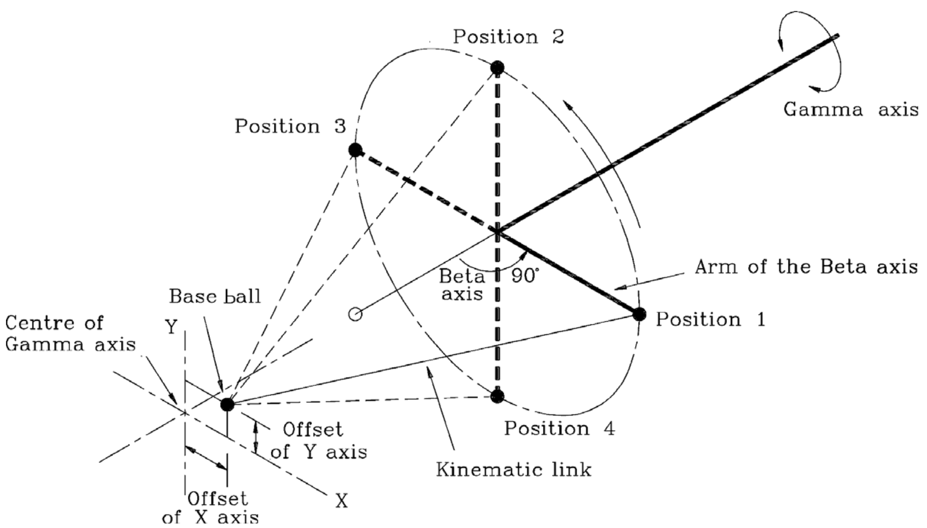

Fig. 4. Setting method of the base ball in the Gamma axis.

https://doi.org/10.1017/S0263574711000130 Published online by Cambridge University Press

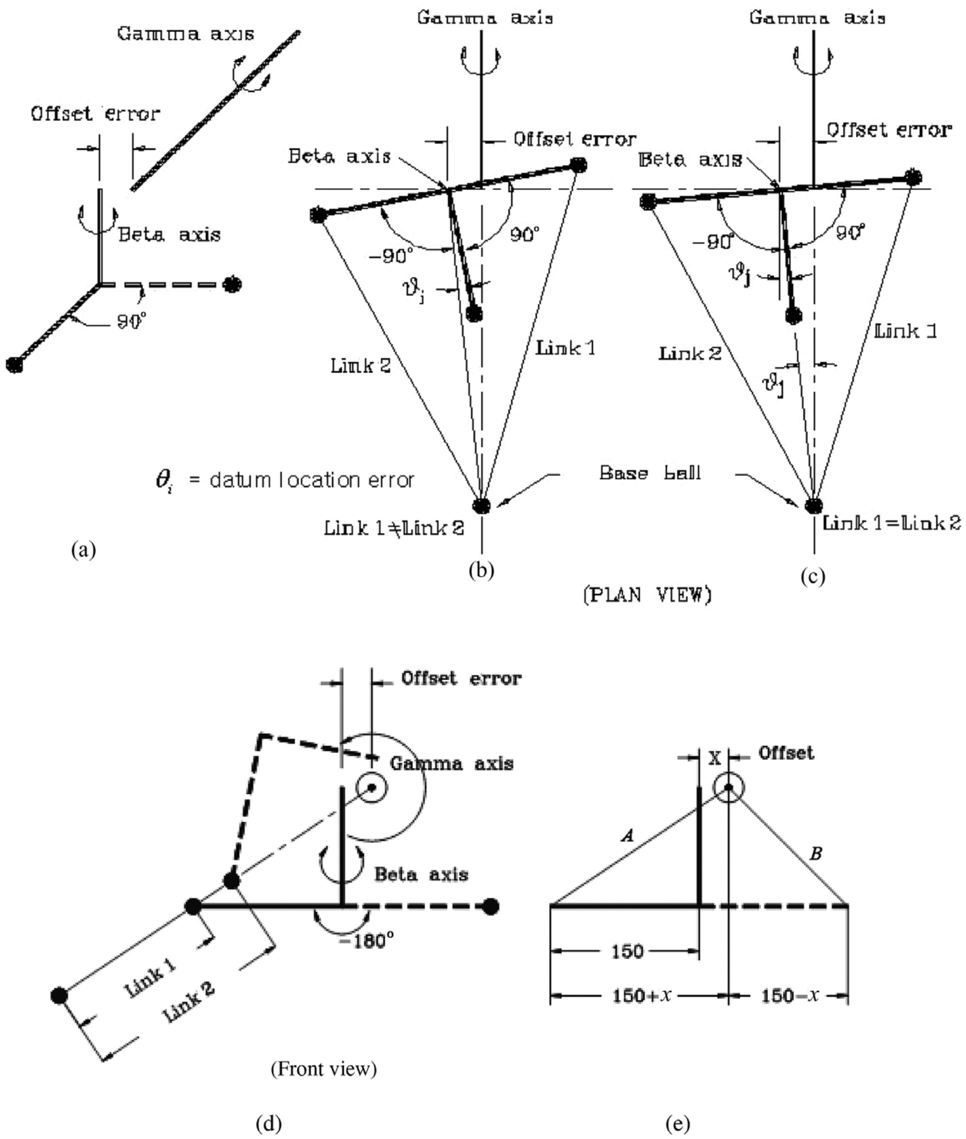

Fig. 5. Geometric error models due to the datum location error and offset error.

Figure 5 shows the configuration of the robot when the arms of the Beta and Gamma axes are parallel. Figure 5(b) which is plan view of Fig. 5(a) shows the error model due to the datum location error of the Beta axis and offset error between the Gamma and Beta axes. Using the kinematic link, the lengths are measured between two balls at the 90° and −90° position of the Beta axis. If the arm of the Beta axis is parallel to the arm of Gamma axis at its zero position and the offset error does not exist, then the kinematic links 1 and 2 should be of same length. If not, the kinematic links 1 and 2 will be of different lengths as shown in Fig. 5(b). The difference in length between kinematic links 1 and 2 will correspond to a datum location error of the Beta axis and the offset error. To find the datum location error of the Beta axis and the offset error, firstly the arm of the Beta axis is aligned to the base ball at its zero position by the measured length of kinematic links 1 and 2 as shown in Fig. 5(b) also θ_i is calculated with the measured links 1 and 2 as shown in Fig. 5(b). Even though the arm of the Beta axis is aligned to the base ball at its zero position, the arm of the Beta axis is not necessarily parallel to the arm of the Gamma axis due to the offset error as shown in Fig. 5(c).

To define the offset error between the Beta and Gamma axes, the base ball was set to the plane of the front view as shown in Fig. 5(d). Using the kinematic link, the length was measured between the base ball and the ball located at the −90° position of the Beta axis as shown in Fig. 5(d). The Beta axis was rotated by 180° (i.e. 90° the Beta axis). When the ball fixed at the robot was aligned between the base ball and Gamma axis by rotation of the Gamma axis, the minimum reading of the kinematic link was taken. The offset error was defined with the difference reading of the kinematic links as shown in Fig. 5(e). Figure 5(e) shows the mathematical model of the offset error.

From Fig. 5(e),

$$(150 + x)^2 + 100^2 = A^2, \tag{1}$$

$$(150 - x)^2 + 100^2 = B^2, \tag{2}$$

$$A - B = \text{Link } 2 - \text{Link } 1, \tag{3}$$

https://doi.org/10.1017/S0263574711000130 Published online by Cambridge University Press

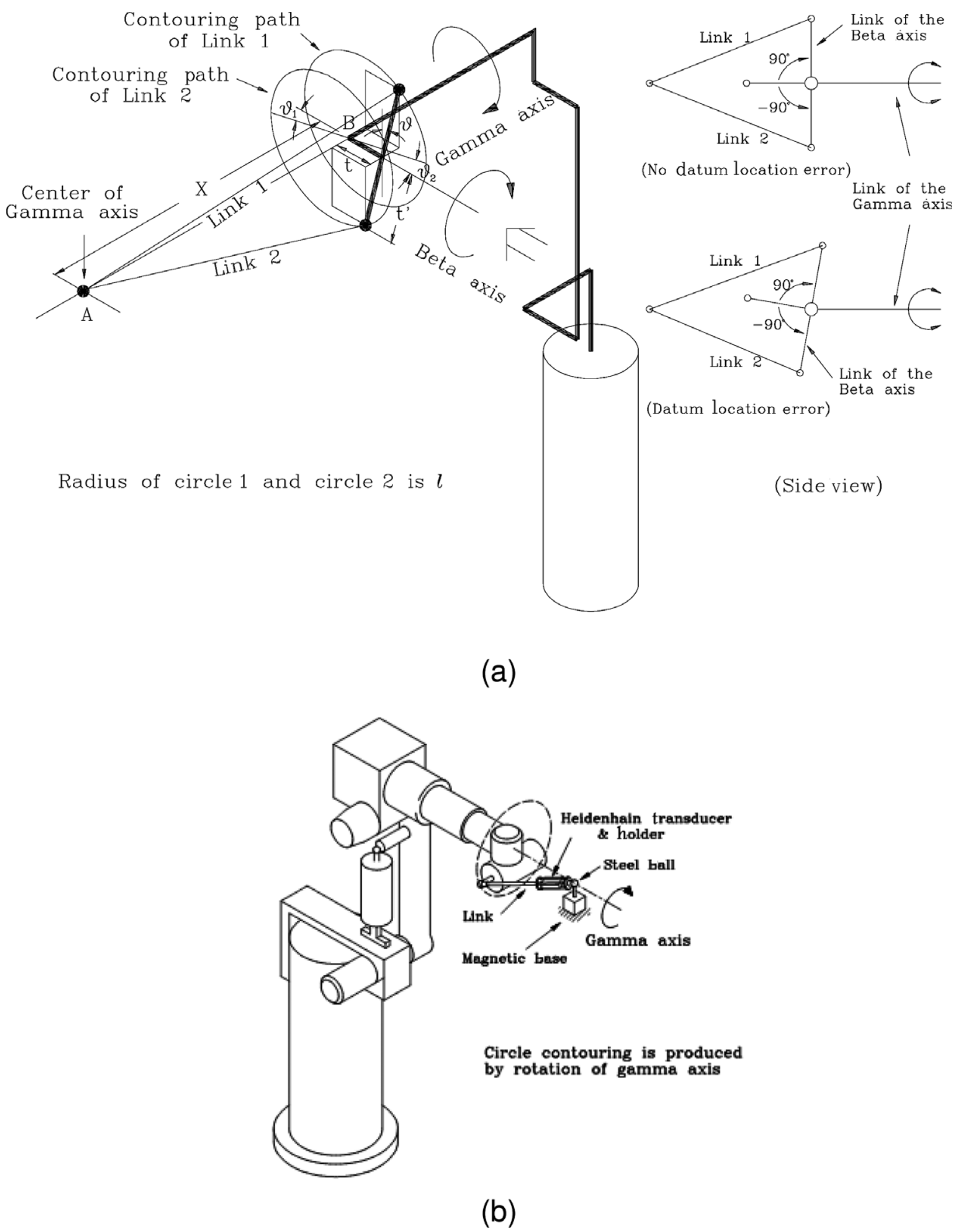

Fig. 6. Geometric model of the datum location error of the Beta axis and equipment setting.

where $A - B$ is the difference reading between the kinematic links.

The offset error(s) between the Beta and Gamma axes are found with Eqs. (1), (2) and (3), also above θ_j is defined with the offset error(s). Therefore the datum location error of the Beta axis corresponds to the combination of the θ_i and θ_j as shown in Fig. 5(b).

3.1.1. Technique to establish Beta axis alignment in the industrial robot. If the Beta axis is aligned to the Gamma axis and the arm of the Beta axis is also parallel to the arm of Gamma axis at zero position of Beta axis, then the kinematic links 1 and 2 should be of the same length at the 90° and −90° of the Beta axis as shown in Fig. 6(a). However if the arm of the Beta axis is not parallel to the arm of Gamma axis at its zero position, then the kinematic links 1 and 2 will be of different lengths as shown in Fig. 6(a). The datum location error of the Beta axis is calculated from the lengths of kinematic links 1 and 2.

From Fig. 6(a),

$$\cos(90 + \theta_1) = (x^2 + l^2 - \text{Link } 1^2)/(2 \cdot l \cdot x), \tag{4}$$

where l is the radius of circle 1 and circle 2,

$$\cos(90 - \theta_2) = (x^2 + l^2 - \text{Link } 2^2)/(2 \cdot l \cdot x), \tag{5}$$

where $\theta_1 + \theta_2 \approx 0$.

Therefore

$$2 \cdot x^2 + 2 \cdot l^2 - \text{Link } 1^2 - \text{Link } 2^2 = 0. \tag{6}$$

https://doi.org/10.1017/S0263574711000130 Published online by Cambridge University Press

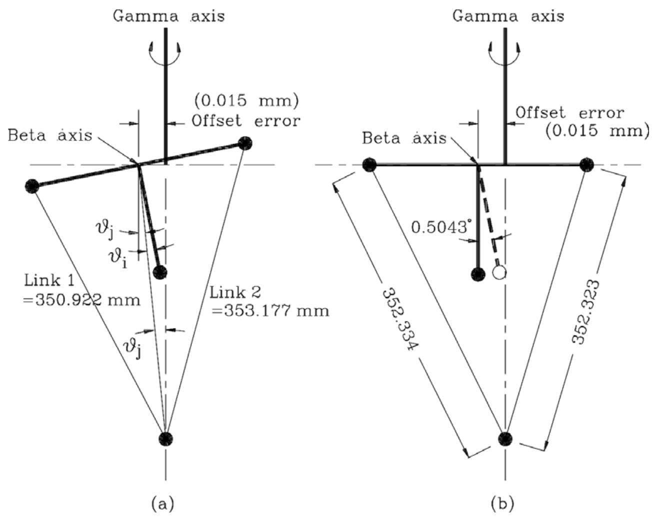

Fig. 7. Experimental result of the datum location error and offset error for the industrial robot.

The distance(s) between points *A* and *B* are found with

$$x = \sqrt{\frac{\text{Link }1^2 + \text{Link }2^2 - 2 \cdot t^2}{2}}, \quad (7)$$

$$(x + t' \cdot \sin\theta_i)^2 + t^2 + (t' \cdot \cos\theta_i)^2 = \text{Link }1^2, \quad (8)$$

$$(x - t' \cdot \sin\theta_i)^2 + t^2 + (t' \cdot \cos\theta_i)^2 = \text{Link }2^2. \quad (9)$$

From the Eqs. (8) and (9),

$$\text{Link }1^2 - \text{Link }2^2 = (x + t' \cdot \sin\theta_i)^2 - (x - t' \cdot \sin\theta_i)^2. \quad (10)$$

Therefore the datum location error of the Beta axis is calculated as

$$\theta_i = \sin^{-1}((\text{Link }1^2 - \text{Link }2^2)/(4 \cdot x' \cdot 150)),$$

where $t' = 150$ from the robot specification.

3.1.2. Experimental determination of the datum location error of the Beta axis in an industrial robot. The datum location error of the Beta axis was determined by an evaluation program, which was based on the mathematical model described in the previous section. Firstly, the offset error between the Beta and Gamma axes was measured with the kinematic link. The 0.015 mm offset error was found with the measuring procedure. To verify θ_i the error of the Beta axis shown in Fig. 5(b), the equipment setting is shown in Fig. 6(b). The kinematic link was attached between the base ball and robot end effector. The base ball was then set to the centre of the Gamma axis by rotating the Gamma axis using the reading of the kinematic link as shown in Fig. 7. The length between the two balls was measured through 360° rotation of the Gamma axis shown in Fig. 6(b), then the Beta axis was rotated by 180° to the −90° position of the Beta axis. The length is again measured by rotating through 360° the Gamma axis at this −90° position of the Beta axis.

The two measured link lengths are different due to the datum location error of the Beta axis and offset error as explained above. The measured lengths of Link 1 and Link 2 are 353.177 mm and 350.922 mm, respectively. The θ_i of Beta axis was calculated using these measured lengths. A 0.5015° of θ_i error is found to exist from the initial position of the Beta axis and a 0.0028° of θ_j error is found with 0.015 mm offset error shown in Fig. 7. Therefore the datum location error of the Beta axis corresponds to the combination of θ_i and θ_j error. A 0.5043° datum location error of the Beta axis was remastered from the initial position of the Beta axis, then the lengths were remeasured at the 90° and −90° of the Beta axis. The result shown in Fig. 7 indicates that by compensating −0.5043° of the Beta axis the link lengths were slightly different due to the offset error. Also the datum location error of the Gamma axis can be measured with trammelling techniques. A 0.1626° of datum location error is measured.

3.2. *Circular contouring test*

3.2.1. Principle of the datum location error of the U axis. Though the datum location error of the wrist part of the robot (Beta and Gamma axes) was evaluated, the error factor still exists in the circle contouring due to the datum location error of the U axis in Fig. 8(a). Usually the angle between the arms of the U and W axes is a right angle in the robot configuration. The datum location error of the U axis can be evaluated by analysis of the shape and the error band in the circular contouring. If the datum location error of the U axis exists, i.e. the arm angle between the link of the W and U axes is not a right angle in the robot configuration in Fig. 8(a), then the shape of the circle is changed to an elliptical shape, the aspect of which is dependent on the datum location error value of the U axis. Also the least squares circle and the error band are dependent on the datum location error value of the U axis.

The industrial robot is usually set to 90° between the links of the W and U axes by a displayed mark point and consequently it is unlikely to be exactly square. If the setting angle between the links of the W and U axes is more than 90° in Fig. 8(a), i.e. the datum location error of the U axis is a positive value, the major axis of the circle is extended in the second and the fourth quadrant and is not exactly elliptical, i.e. the diameter of contouring at the second and the fourth quadrant is longer than the other diameter as shown in Fig. 8(b). If the setting angle between the links of the W and U axes is less than 90°, i.e. the datum location error of the U axis is a negative value, the opposite situation occurs as shown in Fig. 8(b). This simulation in Fig. 8(b) shows the effect of ±0.25° of datum location error of the U axis when the circle of 200 mm radius is generated. If the datum location error of the U axis has a positive angle error, the least squares circle is greater than the nominal circle. If the datum location error of the U axis is a negative angle error, the least squares circle is less than the nominal circle. But the error band is almost the same.

Figure 8(c) shows the relationship between the datum location error of the U axis and the least squares circle. Additionally there is a relationship between the datum location error of the U axis and subsequent error band. An increase in the absolute value of the datum location error of the U axis will produce an error band of the circle which will be proportionally larger. With this simulation data, the least

https://doi.org/10.1017/S0263574711000130 Published online by Cambridge University Press

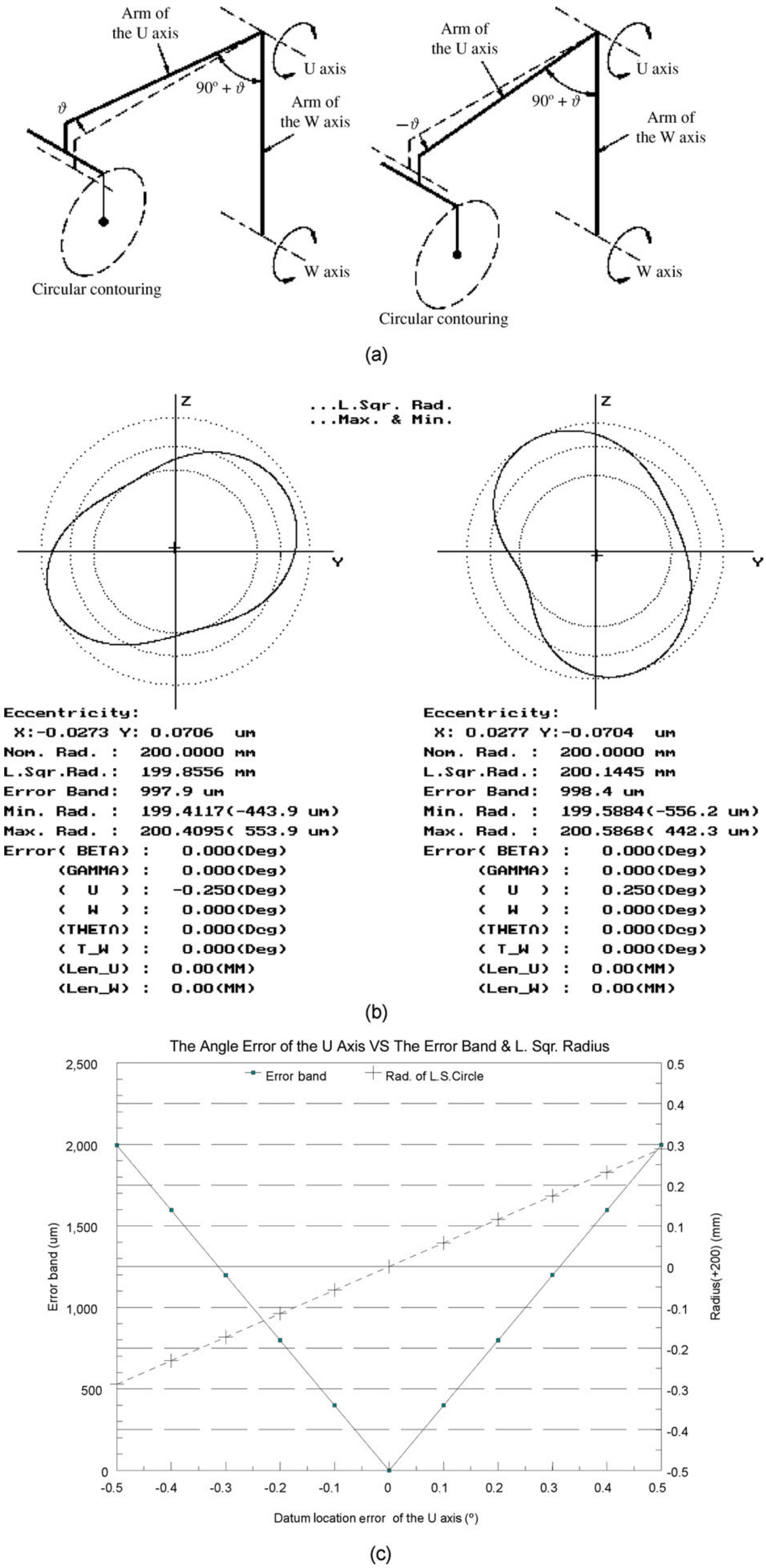

Fig. 8. Simulation result of the error configuration and relationship between the error band and least square circle in the datum location error of the U axis.

https://doi.org/10.1017/S0263574711000130 Published online by Cambridge University Press

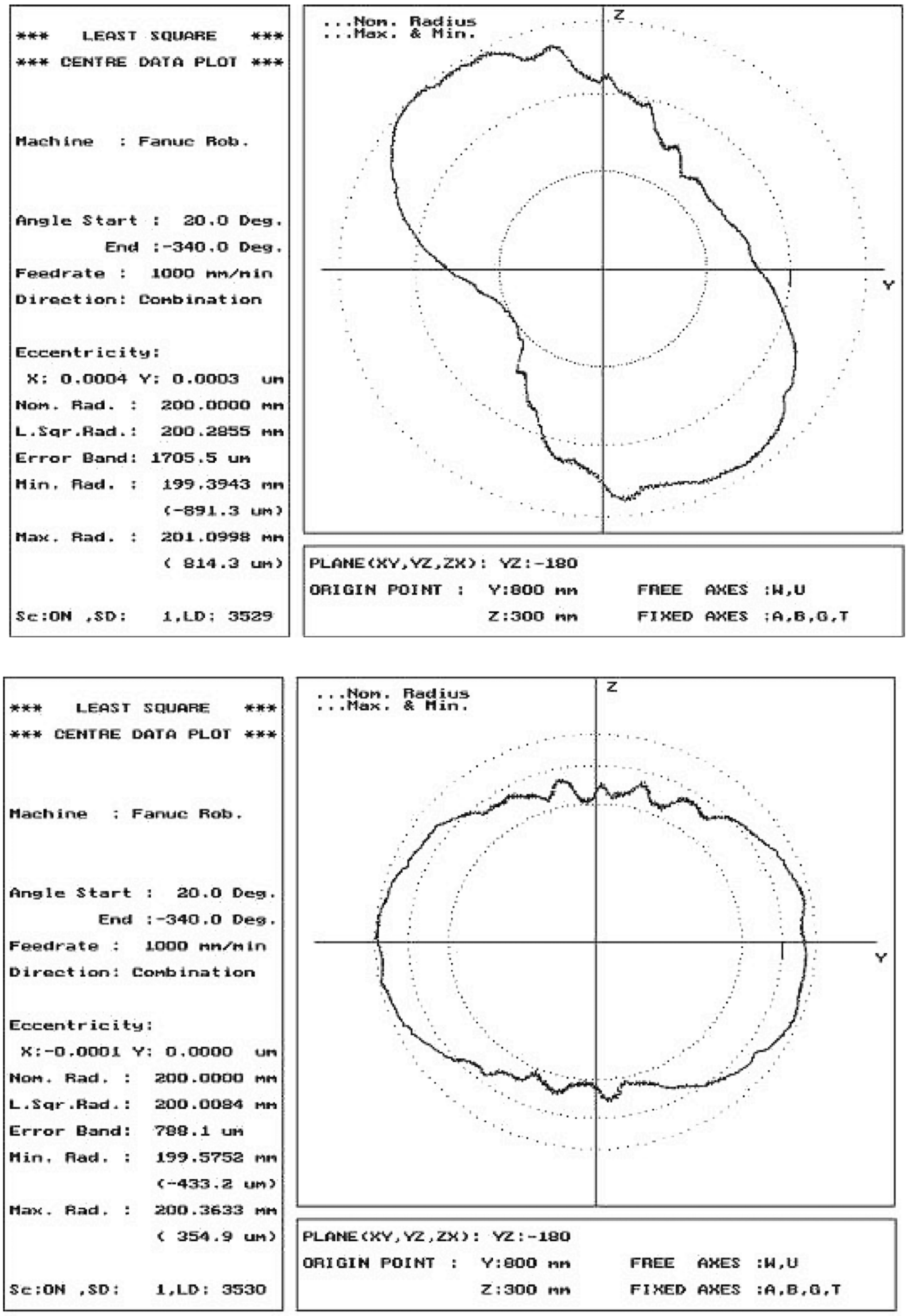

Fig. 9. Experimental data with ±0.25° of datum location U axis error.

squares lines are plotted on the graph of the error band and the datum location error of the U axis. It can be seen that the intersection point of the two least squares lines is optimal at zero degrees datum location of the U axis. Practically the datum location error of the U axis can be found by changing the initial setting angle of the U axis.

3.2.2. Experimental determination of the datum location error of the U axis in the industrial robot. The optimum position of the U axis could be found by changing the initial position of the U axis. After changing the initial position of the U axis, circle contouring is generated by robot operation with the W and U axes, and the circle radius is measured. When the initial position of the U axis was changed by 0.25°, the circle shows an elliptical shape as shown in Fig. 9. Comparing this shape with the simulation data shown in Fig. 8(b), the shape is almost identical and the major axis of the circle is in the second and the fourth quadrant. Note that the fluctuation at 90° and 270° in the experimental data is due to the gear transmission error of the W and U axes. Also the backlash points, at 26.6°, 157.0°, 206.6° and 323.5° on the circle are significantly smaller than compared with the error band. Therefore the gear transmission error of the W and U axes should be subtracted from the experimental data to obtain the actual datum location U axis error. Figure 10 shows the effect after compensation of the gear transmission error of the W and U axes. The

https://doi.org/10.1017/S0263574711000130 Published online by Cambridge University Press

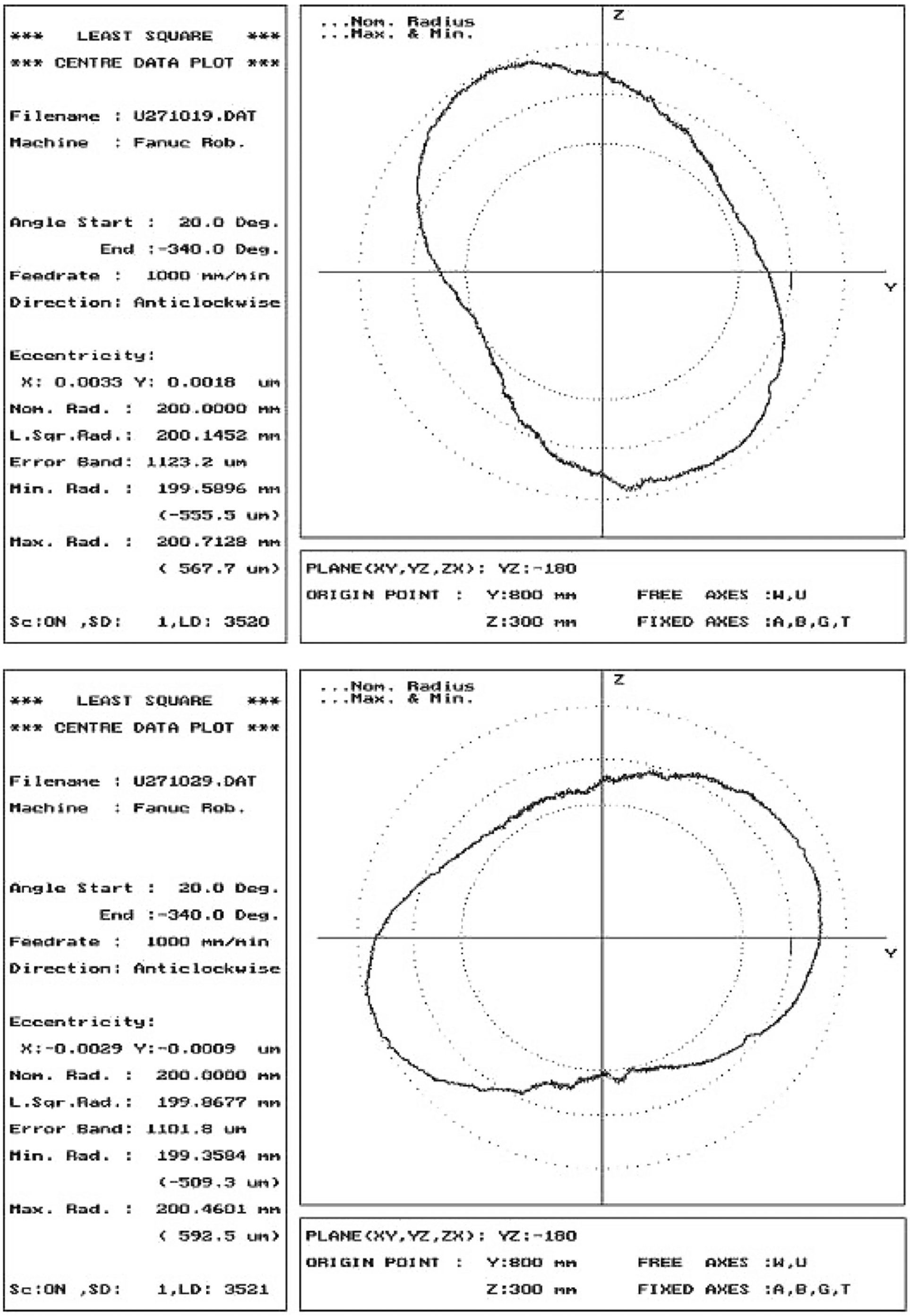

Fig. 10. Experimental result after compensation for the gear transmission error of the W and U axes.

fluctuations previous evident at 90° and 270° are almost eliminated. Comparison of Figs. 8(b) and 10 shows that the least squares circle, the error band and the circle shape are almost similar.

The initial position of the U axis was changed by −0.25°, and the circle radius measured. The result is shown in Fig. 9. Again by comparing the simulated theoretical error (Fig. 8(b)) with the experimental error (Fig. 9), the circle is seen to have an elliptical shape but with a different direction of major axis. Part of this difference is due to the gear transmission error of the W and U axes. It can also be seen that the least squares circle and error band are different. Figure 10 shows the result after compensation for the gear transmission error of the W and U axes. Comparison of Figs. 9 and 10 shows an increase in the error band whilst the least squares circle is decreased. However Fig. 10 looks similar to Fig. 8(b).

A graph, which shows the expected error band versus the datum location angle error of the U axis, is shown in Fig. 11. The experimental data are marked with a diamond and exhibits a curved shape with a minimum error at −0.15° datum location error of the U axis before compensating the gear transmission error of the W and U axes. The rectangular marks on Fig. 11 show the expected errors after compensation for the gear transmission error of the W and U axes. Two least squares lines can be found with the rectangular mark plot; the intersection point of these lines

https://doi.org/10.1017/S0263574711000130 Published online by Cambridge University Press

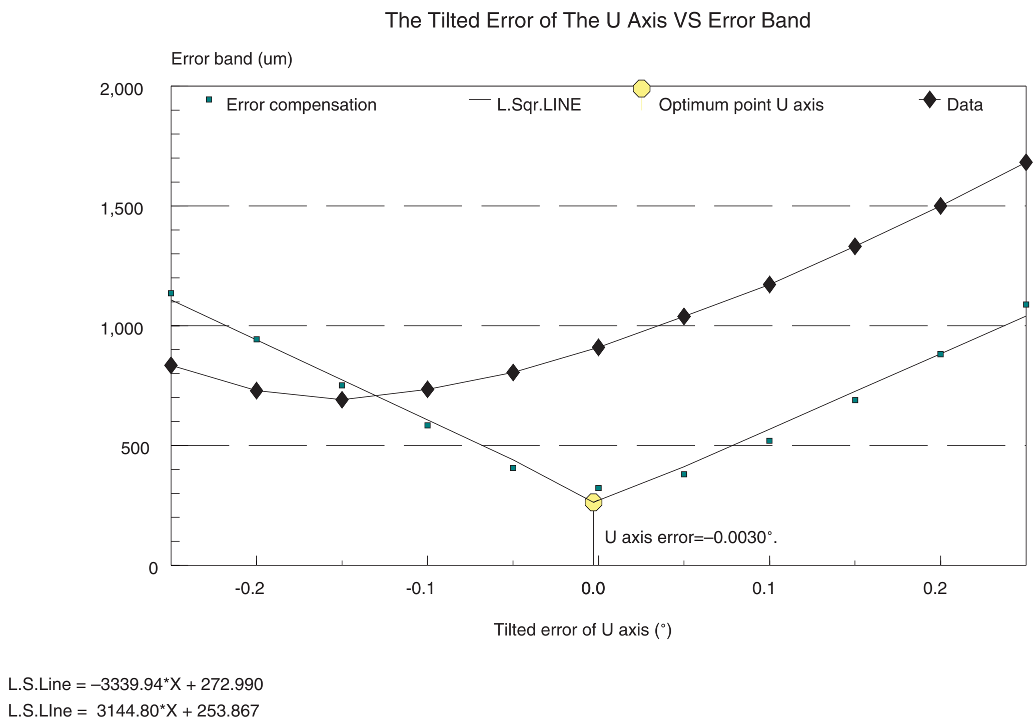

Fig. 11. Experimental result of the relationship between the datum location error versus the error band.

is the optimum zero degrees position of the U axis. From Fig. 11, it can be shown that the optimum zero degrees angle of the U axis is $-0.003°$ from the initial position of the U axis, i.e. the datum location error of the U axis is $-0.003°$.

4. Conclusions

The following conclusions can be drawn from the investigation on robot accuracy performance. Parametric error components of an industrial robot can be established using a ball-bar link with extended range. Circular test data, used in conjunction with simulation of the robot geometry, is a variable technique for characterising the robot error in terms of datum location error and backlash error. Experimental investigation on the test robot by using the procedures developed in the paper shown that significant error components resulted from datum location error. The error resulting from these datum location errors can be minimised by the procedure and technique proposed.

References

1. H. V. Brussel, “Evaluation and testing of robots,” *Ann. CIRP* **39**(1), 657–664 (1990).
2. K. Lau and J. Hocken, “A survey of current robot metrology methods,” *Ann. CIRP* **32**(2), 485–488 (1984).
3. H. J. Warnecke, M. Weck, B. Brodbeck and G. Engel, “Assessment of industrial robots,” *Ann. CIRP* **29**(1), 391–396 (1980).
4. R. H. McEntire, “Three dimensional accuracy measurement methods for robots,” *Ind. Robot* **3**, 105–112 (1976).
5. P. G. Ranky, “Test method and software for robot qualification,” *Ind. Robot* **11**(2), 110–118 (1984).
6. D. L. Riley, “Robot Calibration and Performance Specification Determination,” *Proceedings of the 17th International Symposium on Industrial Robots*, Chicago, Illinois (Apr. 1987) pp. 10–1/17.
7. T. Fohanno, “Assessment of mechanical performance of industrial robots,” *International Symposium on Industrial robots, 12the Proceeding, and 6th International Conference on Industrial Robot Technology*, Paris, France (Jun. 9–11, 1982) pp. 349–358.
8. K. Lau, R. Hocken and W. Haight, “Automatic laser tracking interferometer system for robot metrology,” *Precis. Eng.* **8**(1), 3–8 (1986).
9. J. B. Bryan, “A simple method for testing measuring machines and machine tools, Part 1: Principles and applications,” *Precis. Eng.* **4**(2), 61–69 (1982).
10. N. Vira and K. Lau, “Design and Testing of an Extensible Ball Bar for Measuring the Positioning Accuracy and Repeatability of Industrial Robots,” *Proceedings of the 14th North American Manufacturing Research Conference*, Minnesota (1986) pp. 583–590.
11. A. Slocum and A. Donmez, “Kinematic coupling for precision fixture-Part 2-experimental determination of repeatability and stiffness,” *Precis. Eng.* **10**(3), 112–115 (1988).
12. G. Schlesingler, *Testing Machine Tools* (Pergamon Press, Oxford, England 1978) .
13. J. Park, Assessment of Machine Tool Accuracy Testing Device for Machine Tools *Ph.D. Thesis* (Manchester, England UMIST, 1989).
14. W. Jywe, A Computer-Aided Accuracy Testing Device for Machine Tools *Ph.D. Thesis* (Manchester, England UMIST, 1992).
15. Y. T. Oh, Evaluation of the Accuracy Performance of the Industrial Robots *Ph.D. Thesis* (Manchester, England UMIST, 1997).
16. H. Chen, T. Fuhlbrigge, S. Choi, J. Wang and X. Li, “Practical Industrial Robot Zero Offset Calibration,” *Automation Science and Engineering, 2008. CASE 2008. IEEE International Conference*, Arlington, VA (2008) pp. 516–521.
17. S. Lei, L. Jingtai, S. Weiwei, W. Shuihua and H. Xingbo “Geometry-Based Robot Calibration Method,” *Robotics and Automation, 2004, Proceedings, ICRA ’04, 2004 IEEE International Conference*, vol. 2 (2004) pp. 1907–1912.